

Epidithiodiketopiperazine Biosynthesis: A Four-Enzyme Cascade Converts Glutathione Conjugates into Transannular Disulfide Bridges**

Daniel H. Scharf, Pranatchareeya Chankhamjon, Kirstin Scherlach, Thorsten Heinekamp, Karsten Willing, Axel A. Brakhage, and Christian Hertweck*

A broad range of toxic fungal secondary metabolites that have been implicated in human, animal, and plant diseases share a diketopiperazine scaffold that is overarched by a disulfide bridge.^[1,2] From a pharmaceutical point of view, these epidithiodiketopiperazines (ETPs) have potential therapeutic value because of their efficient suppression of cell proliferation.^[3] In all cases, the biological activity of ETPs critically depends on the structurally intriguing transannular disulfide bridge. This signature residue for ETPs inactivates various proteins by thiol conjugation and generates reactive oxygen species by redox cycling.^[4] Gliotoxin (**1**, Figure 1 A), the archetypal ETP, has been in the focus of research, since it has been implicated as a virulence factor of *Aspergillus fumigatus*, which is a human fungal pathogen causing life-threatening systemic mycoses.^[5] During the past years, individual steps in the gliotoxin biosynthetic pathway have been elucidated at the genetic and biochemical levels. It has been shown that the core of this molecule is assembled by a nonribosomal peptide synthetase, GliP.^[6–9] Promoted by a hydroxylase (GliC) and a glutathione-S-transferase (GliG), the diketopiperazine then undergoes attack of a sulfur nucleophile.^[10,11] By in vitro analyses we have also demonstrated that a dedicated C–S lyase (GliI) cleaves an intermediary biscysteine adduct **2** to yield a dithiol **3**, which is

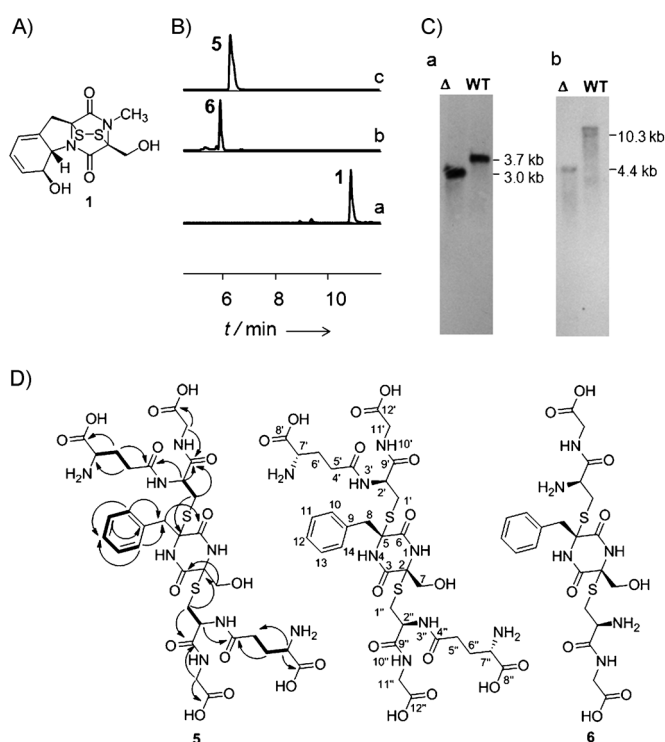


Figure 1. A) Structure of gliotoxin (**1**). B) HPLC–MS profiles of the wild type (a), the $\Delta gliI$ mutant (b), and the $\Delta gliK$ mutant (c). C) Southern blot showing successful deletion of *gliK* (a) and *gliI* (b) genes in the genome of *A. fumigatus*. D) Structure of bisglutathione adduct **5** and key HMBC and COSY correlations; and structure of **6**.

eventually oxidized to the disulfide **4** by an oxidase, GliT (structures of **2–4** are shown in Figure 4).^[12–14] Nonetheless, the structure of the natural S-nucleophile has not yet been unequivocally corroborated, and its enzymatic conversion into the biscysteine adduct has remained fully elusive. Here we solve this riddle by the full characterization of the sulfur-bearing key intermediate as well as genetic and in vitro enzyme analyses. We also report the successful reconstitution of a four-enzyme cascade to yield an intact ETP in a one-pot reaction.

From pathway dissections, enzymatic transformations and MS data we have inferred earlier that a bisglutathione conjugate **5** would represent the first sulfur-bearing intermediate. To reveal enzymes that could catalyze the sequential cleavage of the S-adduct we analyzed the *gli* gene locus and related ETP biosynthesis gene clusters. We identified two

[*] Dr. D. H. Scharf,^[†] P. Chankhamjon,^[†] Dr. K. Scherlach, Dr. T. Heinekamp, K. Willing, Prof. Dr. A. A. Brakhage, Prof. Dr. C. Hertweck
Depts. of Molecular and Applied Microbiology, Biomolecular Chemistry, and Bio Pilot Plant, Leibniz Institute for Natural Product Research and Infection Biology, HKI
Beutenbergstrasse 11a, 07745 Jena (Germany)
E-mail: Christian.Hertweck@hki-jena.de
Prof. Dr. A. A. Brakhage, Prof. Dr. C. Hertweck
Friedrich Schiller University, Jena (Germany)

[†] These authors contributed equally to this work.

[**] We thank A. Perner for MS measurements, M. Poetsch for MALDI measurements, S. Fricke and C. Schult for technical assistance, P. Berthel for performing fermentations, M. Steinacker for downstream processing, P. Hortschansky for support in protein production, and A. Thywißen for providing the fluorescence microscope picture for the table of contents entry. This work was supported by the “Pakt für Forschung und Innovation” of the Free State of Thuringia and the BMBF, and the International Leibniz Research School for Biomolecular and Microbial Interactions (ILRS), as part of the excellence graduate school Jena School for Microbial Communication (JSMC).

Supporting information for this article is available on the WWW under <http://dx.doi.org/10.1002/anie.201305059>.

candidate genes that code for GliK and GliJ, which show similarity to γ -glutamate cyclotransferases and dipeptidases. Notably, homologues of these enzymes are typically involved in primary metabolism. To investigate the role of the enzymes in the gliotoxin pathway we aimed at constructing *gliK* and *gliJ* deletion mutants (Δ *gliK* and Δ *gliJ*) of *A. fumigatus*. We succeeded in generating the targeted knockouts by using a split-fragment PCR-based strategy.^[15] Overlapping ends to the pyrithiamine resistance cassette were introduced at the 3' end of the upstream flanking region and at the 5' end of the downstream flanking region of the respective genes. These constructs were used for protoplast-mediated transformation of *A. fumigatus*. The altered genotype of the mutants was proven by Southern blot analysis (Figure 1C). HPLC–MS monitoring of the Δ *gliK* and Δ *gliJ* mutant cultures showed that gliotoxin biosynthesis was completely abrogated as a result of these mutations (Figure 1B). We thoroughly examined the Δ *gliK* and Δ *gliJ* mutant culture extracts using HPLC–MS and detected trace amounts of two new compounds, **5** and **6**, with m/z 843 ($[M-H]^-$) and m/z 587 ($[M+H]^+$; Figure 1B). HR-ESI-MS data revealed the molecular formula of $C_{32}H_{40}N_8O_{15}S_2$ for **5** and $C_{22}H_{31}N_6O_9S_2$ for **6**. These data and the HR-MSⁿ fragmentation patterns are in perfect agreement with the proposed structures of a bisglutathione conjugate and the corresponding dipeptide (Cys–Gly) adduct (Figures S9 and S10 in the Supporting Information).^[10,12] Because of the extremely high polarity and the instability of the metabolite, obtaining sufficient amounts of **5** for a full characterization proved to be a major challenge. Eventually, from the pooled mycelia of a 260 L Δ *gliK* mutant culture NMR-pure **5** was obtained by repeated size exclusion chromatography at 4°C. ¹³C NMR and DEPT135 spectra of **5** showed the presence of six amide carbon atoms, an aromatic ring system, four carbonyls, eight methylene carbon atoms and six tertiary carbon atoms (Figure S14 in the Supporting Information). The chemical shifts of 29.7 and 29.3 ppm for C1' and C1'' indicated the proximity of two methylenes to the sulfur atoms. This was corroborated by marked HMBC couplings of H1' to C5 and C9', and H1'' to C2 and C9''. Moreover, we observed correlations of H8 to C9, C10 and C14 as well as to the amide carbon atom C6, thus establishing the assignment of the phenylalanine structure. The hydroxymethyl proton H7 showed HMBC correlations to the amide carbon atom C3 and the quaternary carbon atom C2, which is in full agreement with NMR data of the biscysteine adduct **2**.^[12] Furthermore, we detected HMBC correlations of the methine protons H2' and H2'' with two amide carbons C4', C9' and C4'', C9'', respectively, as well as the correlation of H6' and H6'' to C4', C5', C8' and C4'', C5'', C8'', respectively (Figure 1D). The absolute configuration of the free amino

acids was determined by derivatization with Marfey's reagent (1-fluoro-2,4-dinitrophenyl-5-L-alanine-amide, L-FDAA) and HPLC analyses using conjugates of D- and L-amino acids as references.

Bioinformatic analyses suggested that *gliK* codes for a γ -glutamate cyclotransferase. To investigate the exact biochemical function of GliK, an in vitro study was required. Therefore, we used a synthetic gene, cloned the construct into an *E. coli* expression vector, and introduced it into *E. coli* BL21(DE3) cells for protein overproduction. Maltose-binding protein (MBP)-tagged GliK, which was harvested from the biomass of an *E. coli* culture (1 L), was purified using a dextrin column and treated with TEV protease for tag removal. Notably, GliK is difficult to handle, because it tends to form aggregates with itself and MBP (Figure 2D). For

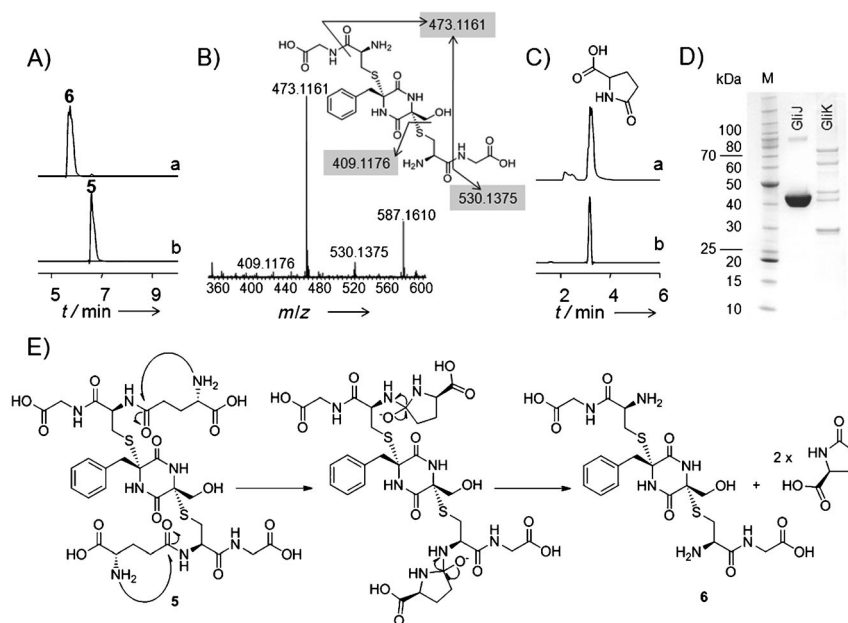


Figure 2. A) HPLC–MS profiles of in vitro biotransformation experiments using a) active GliK and b) heat-inactivated GliK (negative control); **5** (m/z 843; $[M-H]^-$) and **6** (m/z 587; $[M+H]^+$). B) HR-MSⁿ analysis of dipeptide adduct **6**. C) Detection of pyroglutamic acid; a) authentic reference, and b) assay using active GliK. D) Purity of GliK and GliJ analyzed by SDS-PAGE (multiple bands are due to aggregation). E) Model of the bisglutamyl elimination reaction catalyzed by GliK.

purity control we checked all bands on the SDS-PAGE by MALDI-MS (Figures S12, S13 in the Supporting Information) and verified the identity of GliK and MBP in all cases. GliK was then employed in an in vitro assay using **5** as substrate. The course of the reaction was monitored by LC–HRMS, showing that **5** is readily converted into a new product (**6**), which is identical with the compound that accumulates in the Δ *gliJ* mutant. In both cases, MSⁿ fragmentation patterns revealed the sequential loss of glycine and cysteine residues (Figure 2B and Figure S10 in the Supporting Information). Notably, no transformation of **5** could be detected with heat-inactivated GliK (Figure 2A). This finding revealed that **6** is the product of GliK-mediated biotransformation of **5**. A plausible scenario would involve the sequential elimination of two equivalents of glutamic acid from the bisglutathione

intermediate **5**, thus yielding two equivalents of pyroglutamic acid as side product (Figure 2E). To unequivocally prove this postulated route we analyzed pyroglutamic acid formation in the in vitro enzyme assay. Indeed, by HRESI-MS we detected a peak corresponding to pyroglutamic acid with m/z 130.0508 ($[M+H]^+$) (calcd. for $C_5H_8NO_3$ 130.0510), and corroborated its identity through comparison with a synthetic reference compound (Figure 2C). The proposed mechanism is similar to the glutamate cleavage reaction catalyzed by BtrG in butirosin biosynthesis.^[16]

Our next goal was to elucidate the role of the putative dipeptidase GliJ. To clarify the biochemical function of GliJ in vitro, we amplified *gliJ* by using PCR, cloned the amplicon, followed by heterologous production and purification of His₆-tagged GliJ (Figure 2D). Static light scattering experiments revealed the homodimeric status of GliJ (Figure 3D). The theoretical molecular mass of a GliJ dimer is 89.8 kDa, which is in excellent agreement with the measured mass of (83.4 ± 2.1) kDa. Next, we set up the in vitro assay by a sequential enzyme reaction. We hypothesized that GliK might generate **6**, which is the substrate of GliJ and this enzyme would convert the substrate to product **2** with m/z 471 ($[M-H]^-$). Thus, the bisglutathione adduct **5** was added to a mixture of GliK and GliJ, and the course of the reaction was monitored by LC-MS. Whereas no transformation of **5** in the presence of inactivated GliK–GliJ could be detected, we observed con-

version of **5** to **2** (via **6**) with the active enzymes (Figure 3A). The identity of the biscysteine conjugate **2** was unequivocally confirmed by MS-MS (Figure 3B) and comparison with an authentic reference compound.^[12] To verify the postulated release of glycine in the reaction catalyzed by GliK–GliJ we utilized Marfey's reagent. By LC–HRMS we detected a peak [m/z 326.0745 ($[M-H]^-$), calcd. for $C_{11}H_{12}N_5O_7$ 326.0742] that corresponds to the glycine conjugate (FDAA–Gly; Figure 3C), thus further supporting the structure of compound **6**. The enzyme assay showed that GliJ is a peptidase that cleaves off glycine from dipetide conjugate **6** (Figure 3E). We could also show that the activity of GliJ is metal-dependent. Treatment of GliJ with EDTA (2 mM) leads to complete loss of activity and only addition of zinc or manganese ions was sufficient to restore enzyme activity.

With the working enzymes at hand we aimed at reconstituting the entire sequence from the glutathione conjugate to the dithiol and disulfide stage in vitro. Addition of the C–S bond lyase GliI to GliK and GliJ allowed us to convert **5** to the dithiol **3** in a one-pot reaction. Under aerobic conditions we also observed partial conversion of dithiol **3** into the disulfide **4** (Figure 4A). We also succeeded in expanding the cascade by addition of the dithiol oxidase GliT. By means of this four-enzyme mixture, **5** was readily converted into a single product, the ETP **4** in a one-pot reaction (Figure 4B). The identities of all products were unequivocally proven by LC–HRMS, MSⁿ fragmentation patterns, and comparison with authentic references for **3**^[13] and **4**^[12] (Figure S11 in the Supporting Information).

In this study we have elucidated two important and as to date obscure key steps in the biosynthesis of the ETP gliotoxin, a virulence factor of the human pathogen *A. fumigatus*. Large-scale fermentation and laborious purification from a mutant broth unveiled **5** as the first sulfur-bearing intermediate of the gliotoxin pathway. Through in vitro enzyme assays using purified GliK and GliJ we demonstrated that **5** is transformed into **6** by a glutamyltransferase (GliK) and that **6** is subsequently converted to **2** by a metal-dependent dipeptidase (GliJ). Notably, homologues of GliK have only been reported once in the context of natural product biosynthesis, and GliJ is the first dipeptidase involved in a secondary metabolite pathway. Through the successful in vitro reconstitution of a three- (GliKJI) and four-enzyme cascade (GliKJIT) we emulated the whole pathway responsible for dithiol and episulfide formation in the gliotoxin molecule in one pot (Figure 4C). This scheme is particularly interesting, since sulfur incorporation into gliotoxin mirrors mechanisms involved in phase II detoxification of xenobiotics and an alternative glutathione degradation pathway in yeast.^[17,18] Nonetheless, the biochemical functions of the enzymes clearly diverge in primary metabo-

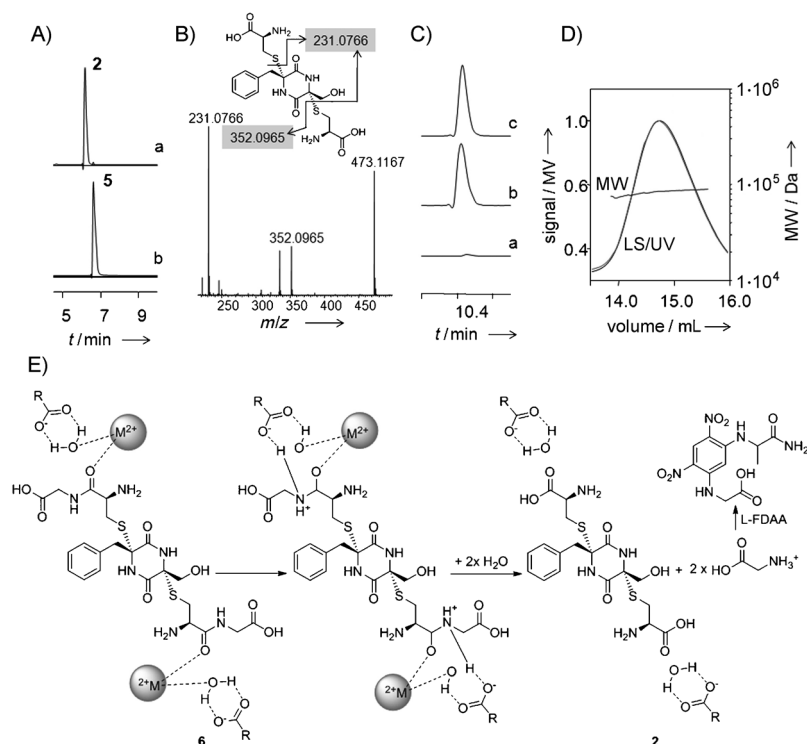


Figure 3. A) HPLC–MS profiles of in vitro biotransformation experiments using a) active GliK–GliJ and b) heat-inactivated GliK–GliJ (negative control). B) HR–MSⁿ analysis of biscysteine adduct **2**. C) HPLC–MS analysis of glycine derivative; a) negative control, b) assay using active GliK–GliJ, and c) synthetic reference for FDAA–Gly. D) Native molecular mass determination of GliJ. LS = light-scattering signal, UV = UV signal, and MW = calculated molecular weight. The LS and UV curves overlap. E) Model for the generation of biscysteine conjugate **2** catalyzed by GliJ.

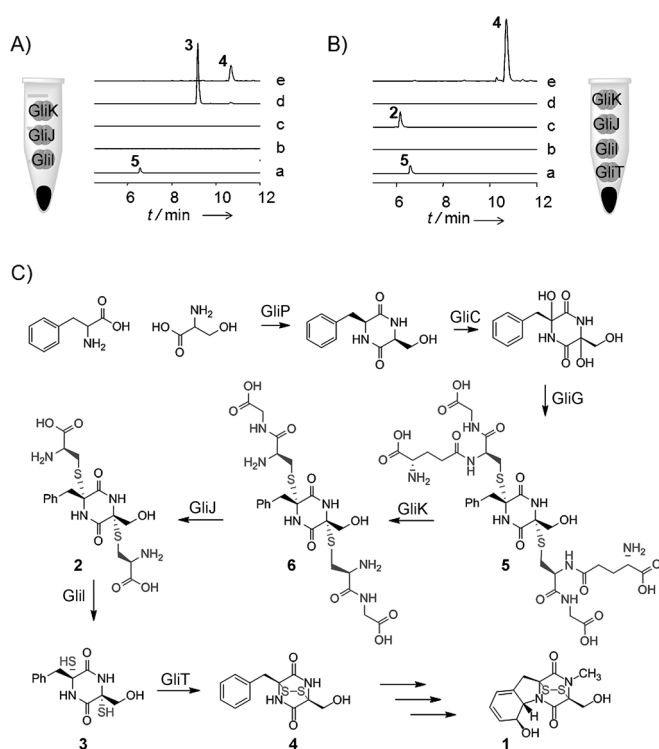


Figure 4. One-pot multienzyme reactions. A) HPLC-MS profiles of biotransformation experiment using GliK-GliJ-GliI, B) HPLC-MS profiles of biotransformation experiment using GliK-GliJ-GliI-GliT. Extracted ion chromatograms: a) **5** (m/z 843; $[M-H]^-$), b) **6** (m/z 587; $[M+H]^+$), c) **2** (m/z 473; $[M+H]^+$), d) **3** (m/z 297; $[M-H]^-$), and e) **4** (m/z 295; $[M-H]^-$). C) Model for gliotoxin biosynthesis showing the dissection of bisglutathione adduct **5** and conversion into an intact ETP.

lism and gliotoxin biosynthesis, where glutathione serves as a sulfur donor. Notably, the normal growth of $\Delta gliK$ and $\Delta gliJ$ with glutathione or Gly-Cys as sole sulfur source shows that these enzymes have no function in primary metabolism. From a mechanistic point of view, the route presented herein complements previously studied microbial sulfur incorporation pathways.^[19–21] The novelty of the fungal pathway is highlighted by the fact that homologues of GliK and GliJ are exclusively encoded in genomes of ETP producers and that the genes for the specialized set of enzymes (GliK-GliJ-GliI-GliT) are a particular trait of all ETP biosynthesis gene clusters. Thus we propose that the enzyme sequence for sulfur incorporation and dithiol/disulfide formation elucidated herein represents a unifying scheme for all ETP pathways, which are widespread among fungi (Figures S16 and S17 in the Supporting Information).^[22] Currently over 50 different fungi, among them many animal or plant pathogens, are supposed to produce ETPs. Whereas some ETPs have been implicated in several animal and plant diseases, some structures are not known to date.^[1,2] Considering the diverse ecological and medicinal roles of ETP toxins, the completion of the sulfur incorporation pathway using gliotoxin biosynthetic enzymes as a model has broad implications. Knowledge on the specialized genes and enzymes will not only allow the identification of potential ETP gene clusters in the genomes

of pathogenic microorganisms, but may also be exploited for engineering potential therapeutics featuring the unusual epidithio pharmacophore.

Received: June 12, 2013

Published online: August 26, 2013

Keywords: *Aspergillus fumigatus* · biosynthesis · dipeptidase · gliotoxin · mycotoxins

- [1] A. D. Borthwick, *Chem. Rev.* **2012**, *112*, 3641–3716.
- [2] D. M. Gardiner, P. Waring, B. J. Howlett, *Microbiology* **2005**, *151*, 1021–1032.
- [3] D. M. Vigushin, N. Mirsaidi, G. Brooke, C. Sun, P. Pace, L. Inman, C. J. Moody, R. C. Coombes, *Med. Oncol.* **2004**, *21*, 21–30.
- [4] P. Waring, A. Sjaarda, Q. H. Lin, *Biochem. Pharmacol.* **1995**, *49*, 1195–1201.
- [5] D. H. Scharf, T. Heinekamp, N. Remme, P. Hortschansky, A. A. Brakhage, C. Hertweck, *Appl. Microbiol. Biotechnol.* **2012**, *93*, 467–472.
- [6] C. J. Balibar, C. T. Walsh, *Biochemistry* **2006**, *45*, 15029–15038.
- [7] C. Kupfahl, T. Heinekamp, G. Geginat, T. Ruppert, A. Hartl, H. Hof, A. A. Brakhage, *Mol. Microbiol.* **2006**, *62*, 292–302.
- [8] R. A. Cramer, Jr., M. P. Gamcsik, R. M. Brooking, L. K. Najvar, W. R. Kirkpatrick, T. F. Patterson, C. J. Balibar, J. R. Graybill, J. R. Perfect, S. N. Abraham, W. J. Steinbach, *Eukaryotic Cell* **2006**, *5*, 972–980.
- [9] S. Spikes, R. Xu, C. K. Nguyen, G. Chamilos, D. P. Kontoyiannis, R. H. Jacobson, D. E. Ejzykiewicz, L. Y. Chiang, S. G. Filler, G. S. May, *J. Infect. Dis.* **2008**, *197*, 479–486.
- [10] D. H. Scharf, N. Remme, A. Habel, P. Chankhamjon, K. Scherlach, T. Heinekamp, P. Hortschansky, A. A. Brakhage, C. Hertweck, *J. Am. Chem. Soc.* **2011**, *133*, 12322–12325.
- [11] C. Davis, S. Carberry, M. Schrettl, I. Singh, J. C. Stephens, S. M. Barry, K. Kavanagh, G. L. Challis, D. Brougham, S. Doyle, *Chem. Biol.* **2011**, *18*, 542–552.
- [12] D. H. Scharf, P. Chankhamjon, K. Scherlach, T. Heinekamp, M. Roth, A. A. Brakhage, C. Hertweck, *Angew. Chem.* **2012**, *124*, 10211–10215; *Angew. Chem. Int. Ed.* **2012**, *51*, 10064–10068.
- [13] D. H. Scharf, N. Remme, T. Heinekamp, P. Hortschansky, A. A. Brakhage, C. Hertweck, *J. Am. Chem. Soc.* **2010**, *132*, 10136–10141.
- [14] For an independent study on GliT see: M. Schrettl, S. Carberry, K. Kavanagh, H. Haas, G. W. Jones, J. O'Brien, A. Nolan, J. Stephens, O. Fenelon, S. Doyle, *PLoS Pathog.* **2010**, *6*, e1000952.
- [15] E. Szewczyk, T. Nayak, C. E. Oakley, H. Edgerton, Y. Xiong, N. Taheri-Talesh, S. A. Osmani, B. R. Oakley, *Nat. Protoc.* **2006**, *1*, 3111–3120.
- [16] N. M. Llewellyn, Y. Li, J. B. Spencer, *Chem. Biol.* **2007**, *14*, 379–386.
- [17] H. Kaur, D. Ganguli, A. K. Bachhawat, *J. Biol. Chem.* **2012**, *287*, 8920–8931.
- [18] A. Pastore, G. Federici, E. Bertini, F. Piemonte, *Clin. Chim. Acta* **2003**, *333*, 19–39.
- [19] A. Braunshausen, F. P. Seebeck, *J. Am. Chem. Soc.* **2011**, *133*, 1757–1759.
- [20] M. F. Freeman, K. A. Moshos, M. J. Bodner, R. Li, C. A. Townsend, *Proc. Natl. Acad. Sci. USA* **2008**, *105*, 11128–11133.
- [21] F. P. Seebeck, *J. Am. Chem. Soc.* **2010**, *132*, 6632–6633.
- [22] N. J. Patron, R. F. Waller, A. J. Cozijnsen, D. C. Straney, D. M. Gardiner, W. C. Nierman, B. J. Howlett, *BMC Evol. Biol.* **2007**, *7*, 174.